

# AN UPDATE ON EIC RAPID CYCLING SYNCHROTRON OPTICS\*

H. Lovelace III<sup>†</sup>, C. Montag, V. Ranjbar, Brookhaven National Laboratory, Upton, NY, USA  
F. Lin<sup>‡</sup>, Oak Ridge National Laboratory, Oak Ridge, TN, USA

## Abstract

The Electron-Ion Collider (EIC) requires continuous replacement of the stored electron bunches to facilitate arbitrary spin patterns in the Electron Storage Ring (ESR). This is accomplished by a dedicated, spin transparent Rapid Cycling Synchrotron (RCS). The dynamic range of the accelerator is from 3 GeV to 18 GeV. To maintain stability throughout the acceleration ramp, the linear and nonlinear optics must be tuned accordingly. In this paper, we will discuss the updated linear optics, chromaticities, and dynamic aperture of the RCS.

## INTRODUCTION

The Electron-Ion Collider project will provide center of mass collision energy above 130 GeV which will reach well into the quark-gluon dominated regime allowing further exploration into the cause of the nucleon mass, nucleon spin, and the properties of dense gluonic systems [1]. The polarization of the electron and hadron beams are crucial to the EIC project. The electron beam is used to probe the heavier nucleons and in polarization studies determine how the sea quark and gluon distributions determine the spin of the nucleon.

The design of the accelerator chain utilizes the existing Relativistic Heavy Ion Collider (RHIC) [2] tunnel and upgraded preinjectors and injectors. The pre-injectors, 200 MeV linear accelerator (LINAC), electron beam ion source (EBIS), and Tandem van der Graaf will provide polarized proton beams generated from the optically pumped polarized ion source (OPPIS) [3], polarized light ions, and unpolarized heavy ions. The beam of ions is injected into and accelerated by the Alternating Gradient Synchrotron (AGS) booster, transferred to the AGS, and then accelerated and transferred to the EIC Hadron Storage Ring (HSR). The HSR design includes the arcs of the existing RHIC and remodeled straight sections.

The electron accelerator chain begins with the 200 MeV electron LINAC that injects into an rapid cycling synchrotron (RCS) booster and accelerated to 3 GeV. The polarized electron beam is then transferred to the RCS and accelerated to an energies up to 18 GeV. After acceleration the beam is then transferred to the Electron Storage Ring (ESR) [4] which shares an interaction point with the HSR with the possibility of a second.

\* Work supported by Brookhaven Science Associates, LLC under Contract No. DE-SC0012704 with the U.S. Department of Energy.

<sup>†</sup> hlovelace3@bnl.gov

<sup>‡</sup> Work supported by UT-Battelle, LLC, under contract DE-AC05-00OR22725

Table 1: Magnet Misalignment Given to Magnetic Elements

<b>Circumference (m)</b>	3844.633
<b>Horizontal Tune, <math>Q_x</math></b>	46.28
<b>Vertical Tune, <math>Q_y</math></b>	46.285
<b>Transition <math>\gamma, \gamma_T</math></b>	41.04
<b>H. Chromaticity, <math>\chi_x</math></b>	1
<b>V. Chromaticity, <math>\chi_y</math></b>	1
<b>Natural emittance (3 GeV), <math>\epsilon_x</math> (nm)</b>	0.65
<b>Number of Dipoles (#)</b>	768
<b>Number of Quadrupoles (#)</b>	530
<b>Number of Sextupoles (#)</b>	414

## RCS LAYOUT

The RCS layout is composed of three lattice types, experimental bypass, non-experimental straight section, and arc. The lattice is designed with 1.9 m dipoles which reach a peak field of 0.26 T. The quadrupoles reach a peak field of 25 T/m with a length of 0.6 m, and an aperture of 40 mm. The FODO cell length in the arc is 12.53 m. The sextupole length is 0.5 m with a peak field at 18 GeV of 172 T/m<sup>2</sup>.

The experimental bypass is composed of 16 dipoles and 32 quadrupoles. A unique feature of the experimental bypass is the two pair of dipoles at near the center of the insertion region (IR) which bends the beam line radially outward to avoid the electron Proton Ion Collider (ePIC) detector experiment. In the region where the detector is housed, a 17 m drift is placed to avoid any field leakage from the quadrupoles from interfering with the detector solenoid field. Figure 1 shows the Twiss parameters of the experimental bypass, dispersion, and layout. In experimental bypass, a sextupole is paired with the QD, QF, QFA, QD1, QF1, QF2, QD2, QD2A, and QF2B quadrupoles.

The non-experimental straight section is composed of 16 dipoles and 34 quadrupoles. The straight section is design to accommodate various configurations. Whether it is the injection or RF area, the optics of this region remain the same. The injection will occur in the 4 o'clock region of the RCS, the same region of the HSR [5]. The three 591 MHz radiofrequency (RF) cavities are located in the 10 o'clock region. Figure 2 is a plot of the optics, dispersion, and layout of the non-experimental straight section. In non-experimental straight section, a sextupole is paired with the QDN, QFN, QDNA, QD1N, QF1N, and QD3N quadrupoles, three less sextupole families than the experimental bypass.

There are 162 FODO cells with 28 cells per arc. The cells come in three different flavors where we have a total 6 sextupole families which is explained in the nonlinear subsection. Each quadrupole in the arc comes as a corrector-quadrupole-sextupole (CQS) package.

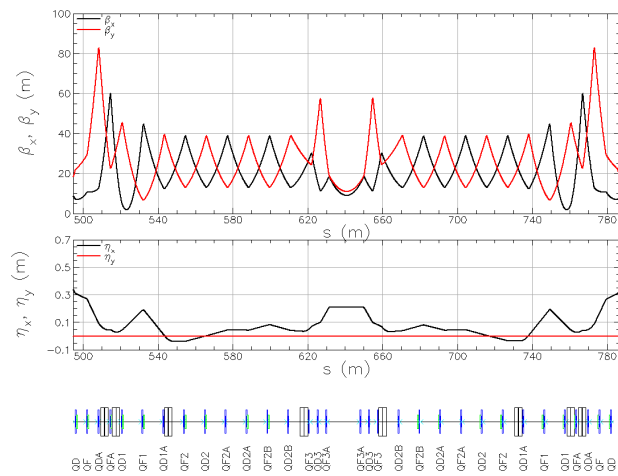


Figure 1: The experimental bypass optics and layout. Top: Twiss parameters, middle: dispersion, and bottom: lattice layout where the black boxes are dipoles, blue boxes are quadrupoles, and the cyan boxes are sextupoles.

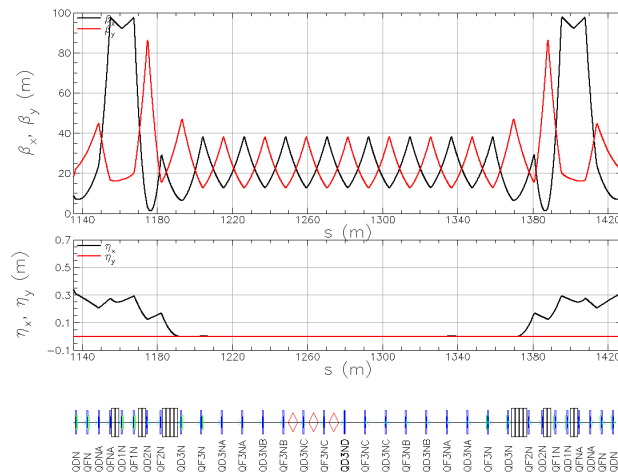


Figure 2: The non-experimental bypass optics and layout. Top: Twiss parameters, middle: dispersion, and bottom: lattice layout where the black boxes are dipoles, blue boxes are quadrupoles, and the cyan boxes are sextupoles. The red diamonds, seen in the layout represent the 591 MHz RF cavities.

## OPTICS

The lattice optics can be separated into two part, linear and nonlinear. The lattice tunes are 46.280 horizontal, and 40.285, vertical. The fractional tune, for both planes, is far enough away from any tune resonances that may inhibit the stable motion of large amplitude particles. Table 1 of lattice parameters.

### Linear

The linear optics are obtain by first setting the arc cell phase advance,  $\phi_{x,y} = 60^\circ$ . The phase advance was chosen to reduce the transition,  $\gamma_T$ , of the lattice while maintaining an average  $\beta$ -function of 13 m in the arcs which keeps

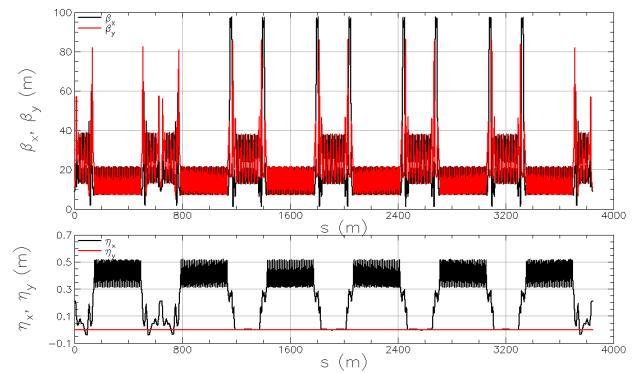


Figure 3: The RCS optics. Top: Twiss parameters and bottom: dispersion.

the lattice below the instability threshold introduced by the impedance [6]. The average  $\beta_{x,y}$  of the lattice is 19.94 m and 20.09 m, respectively. The full lattice optics are shown in Fig. 3. The Bmad accelerator toolkit [7] was used to model the optics of the RCS.

The experimental straight is then optically matched to the half cell at the end of the arc. The dispersion is then controlled and minimized to the FODO cells that span from QD2 to QF2B. This FODO has  $\phi_{x,y} = 30^\circ$  which contributes less to the resonance driving terms than a stronger focusing system. The FODO is then matched to the doublet QF3A which bridges the optics from the forward side of the lattice to the rear. Special care is taken in matching the dispersion derivative to zero at the center of the bypass to prevent the generation of dispersion waves. The rear side is the reflection of the forward.

The non-experimental bypass optics are generated in very much the same way as the experimental straight. The forward side of the lattice is matched to the arc and dispersion is suppressed and optically matched to the FODO cells that span from QD3NA of on the forward side to QD3NA on the rear. The non-experimental straight is also symmetric about the midpoint.

### Nonlinear

With a phase advance close to  $60^\circ$ , the number of sextupole families in the arc is 6 which is standard [8]. The chromaticity is optimized to 1 unit in both planes and the resonance driving terms (RDTs) are acted upon directly. Table 2 list the driving terms minimized during the optimization.

Figure 4 displays the first, second, and third order chromaticities of the RCS. The non-linear chromaticities are relatively small with the second order chromaticity absolute value of less than 100 units. The horizontal higher order chromaticities can be reduced further with the addition of horizontally focusing sextupoles in the non-experimental straight section non-dispersive region.

The effective Hamiltonian,  $h_{xxxx}$ , and the resonance basis can be derived using the methods described in [9–12]. While minimizing the driving terms, W-function [8] is also minimized. Figure 5 displays the W-functions of the RCS

Table 2: Resonance Driving Terms

$h_{20001}$	1.0948
$h_{00201}$	2.9227
$h_{10002}$	0.0885
$h_{21000}$	1.8569
$h_{30000}$	1.3047
$h_{10110}$	1.5822
$h_{10020}$	3.6825
$h_{10200}$	2.5518
$h_{22000}$	1754.2
$h_{11110}$	13268.
$h_{00220}$	856.67
$h_{31000}$	23.713
$h_{40000}$	245.75
$h_{20110}$	171.29
$h_{11200}$	143.30
$h_{20020}$	3747.7
$h_{20200}$	1161.5
$h_{00310}$	433.74
$h_{00400}$	255.32

with a momentum difference of  $1 \times 10^{-4}$  at injection energy. The RDT absolute values and W-function are minimized by the arc geometric sextupoles and the sextupoles in the straight section. The dynamic aperture (DA) is shown in

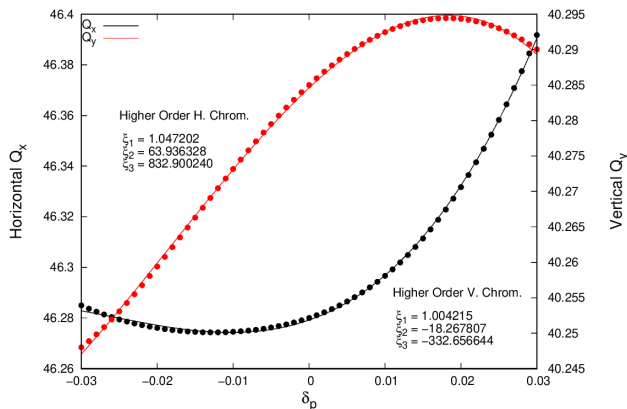


Figure 4: Chromatic scan  $\pm 3\%$   $dp/p$ . The second and third order horizontal chromaticities are: 63.94 and 832.9, respectively. The second and third order vertical chromaticities are: -18.3 and -332.7, respectively.

Fig. 6. The DA for the on momentum particle stretches from  $40\sigma$  horizontally and  $45\sigma$  vertically. The beam size at the observation point is  $295.9\ \mu\text{m}$ , horizontally and  $508.8\ \mu\text{m}$ , vertically. The momentum aperture extends to  $\pm 2.5\ dp/p$ . The DA was scanned for 7 different phase angles spaced  $25.7^\circ$  apart.

## CONCLUSION

The linear optics, chromaticities, and dynamic aperture for the RCS are presented. The linear optics have an average  $\beta$ -function approximately 20 m in both planes with working

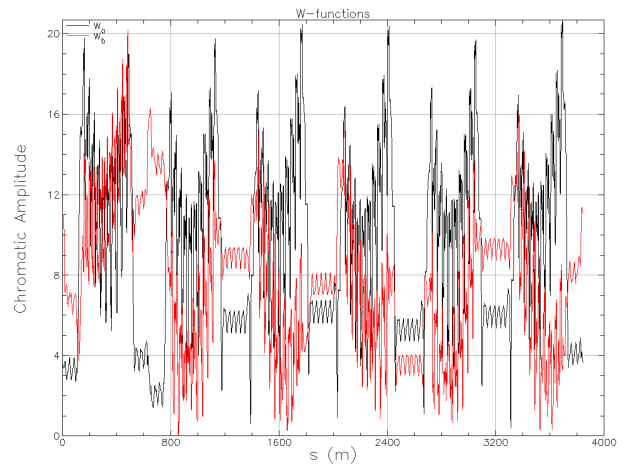


Figure 5: The W-function of the RCS.

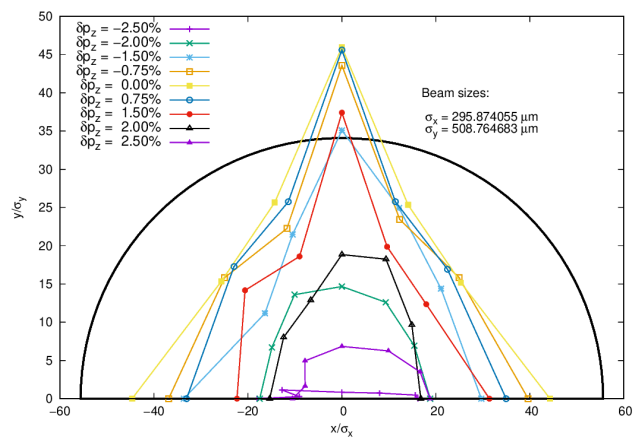


Figure 6: The dynamic aperture of the RCS for  $\pm 2.5\%$   $dp/p$ . The solid black curve is the aperture of the beam pipe with diameter 32.9 mm.

points 46.280 and 40.285, horizontal and vertical, respectively. The  $\gamma_T$  of the lattice is 41.04. The linear chromaticity is 1 unit in both planes with second order chromaticities no exceeding 100 and third order not exceeding 1000. The dynamic aperture is  $40\sigma$  horizontally and  $45\sigma$  vertically.

## FUTURE WORK

The RCS needs a study on polarization transmission. Preliminary study shows 99% polarization transmission, however, only with intrinsic resonances included. With the inclusion of offsets in the quadrupole magnets, a study on the effect of the imperfection resonances may be performed. In addition to polarization studies, magnet field errors need to be included.

## ACKNOWLEDGEMENTS

We would like to thank the RCS Beam and Polarization Dynamics group for aiding in the development of the RCS. We thank the RCS mechanical engineering group for providing guidelines on the layout of the RCS.

## REFERENCES

- [1] *Electron-Ion Collider at Brookhaven National Laboratory Conceptual Design Report*, Collider-Accelerator Department, Upton, NY, Oct. 2020.
- [2] *RHIC: relativistic hadron ion collider configuration manual*, Collider-Accelerator Department, Upton, NY, Nov. 2006.
- [3] A Zelenski, “High-intensity polarized H-(proton), deuteron and 3He++ ion source development at BNL”, Brookhaven National Lab. (BNL), Upton, NY (United States), Rep. BNL-79940-2008-CP, June 2008. <https://www.osti.gov/biblio/933081>
- [4] D. Marx *et al.*, “Lattice design of the EIC electron storage ring for energies down to 5 GeV”, in *Proc. IPAC’23*, Venice, Italy, Sep. 2023, pp. 104–107. doi: 10.18429/JACoW-IPAC2023-MOPA037
- [5] H. Lovelace III *et al.*, “Lattice optimization for Electron Ion Collider Hadron storage ring injection”, in *Proc. IPAC’23*, Venice, Italy, Sep. 2023, pp. 519–522. doi: 10.18429/JACoW-IPAC2023-MOPL008
- [6] M. Blaskiewicz *et al.*, “Recent Beam Stability Analysis for the EIC”, Dec. 2023. doi: 10.2172/2311086
- [7] D. Sagan, “Bmad: A relativistic charged particle simulation library”, *Nucl. Instrum. Meth.*, vol. A558, no. 1, pp. 356–359, 2006. doi: 10.1016/j.nima.2005.11.001
- [8] Brian William St. Leger Montague, “Chromatic effects and their first-order correction”, in *CAS - CERN Accelerator School : Accelerator Physics*, Oxford, UK, Sep. 1985, pp. 75–90. doi: 10.5170/CERN-1987-003-V-1.75
- [9] André Deprit, “Canonical transformations depending on a small parameter”, *Celestial mechanics*, vol. 1, no. 1, pp. 12–30, Mar. 1969. doi: 10.1007/BF01230629
- [10] J. Bengtsson, “The Sextupole Scheme for the Swiss Light Source (SLS): An Analytic Approach”, Paul Scherrer Institut (PSI), Villigen, Switzerland, Rep. SLS Note 9/97, Mar. 1997.
- [11] C-X Wang, “Explicit formulas for 2nd-order driving terms due to sextupoles and chromatic effects of quadrupoles”, Argonne National Lab. (ANL), Argonne, IL (United States), Rep. ANL/APS/LS-330, Apr. 2012. doi: 10.2172/1039519
- [12] Henry Lovelace III and J. Kewisch, “A Damping Ring for the Rapid Cycling Synchrotron”, Brookhaven National Laboratory (BNL), Upton, NY (United States), Rep. BNL-224949-2023-TECH, Oct. 2023. doi: 10.2172/2204617